中国激光

铜微纳结构的激光直写及其应用研究进展

周兴汶，廖嘉宁，姚煜，康慧，郭伟，彭鹏*

北京航空航天大学机械工程及自动化学院，北京 100191

摘要 电性能优良且成本低廉的铜微纳结构在柔性电子领域中展现出广阔的应用前景。激光直写因其快速灵活且可控性高等优势，成为铜微纳结构的高效加工方法之一。概述了微纳结构激光加工的技术特点，随后针对激光直写铜微纳结构展开论述。重点分析了前驱体成分及激光工艺参数对铜微/纳观结构及电性能的影响，探讨了激光直写在铜微纳结构可控制备中的优势。列举了所得结构在柔性电子器件制造中的典型应用场景，分析了典型器件的工作机理。此外，对激光直写微纳结构的未来发展趋势进行了展望。

关键词 激光制造；激光材料加工；纳米材料；纳连接；柔性电极

中图分类号 TN249 **文献标志码** A **doi**：10.3788/CJL202148.0802012

1 引 言

相对于传统电子，新兴的柔性电子具有更大的灵活性，能够在一定程度上适应不同的工作环境，满足设备的形变要求，在无线通信、多功能娱乐、个人医疗保健等多个方面有着广泛的应用[1-2]。典型的柔性电子系统由导电结构及功能结构组成，其中，功能结构通过可变的电性能对外部环境如应力、应变、温度、化学介质等进行响应；导电结构用于传输电力及响应信号。理想的器件可连续、稳定、密切地监测人类/机械活动而不会对其造成干扰或产生限制[3]，因而对器件的材料性能有着极高要求。

具有独特物理化学性质的纳米材料在柔性电子领域应用广泛。对于导电结构，贵金属纳米材料（如金、银、铂等）因其优良的导电性及化学稳定性而备受关注[4-6]。然而，贵金属纳米材料的资源有限且成本高昂，限制了其在大规模柔性电子生产中的应用。铜（Cu）因其资源丰富（较银产能高 1000 倍）、成本低（约为银价格的 1%）、固有导电性高（略低于银，且比金高）等优点，有望取代贵金属纳米材料，继而降低导电结构的制造成本[7]。此外，铜氧化物（氧化铜及氧化亚铜）纳米结构为重要的半导体，常作为功能结构集成到微电子器件中[8-10]。纳米材料的制造可分为“自上而下”和“自下而上”两类工艺。其中，“自下而上”工艺的材料利用率高，能精细地调控微纳结构，具有更低的制造成本[6]。在传统的“自下而上”过程中，首先基于“湿化学法”（例如水热法、化学沉淀法等）完成纳米材料的合成。通过对溶液成分、pH 值、环境温度等反应条件进行调控，可以精确地控制所得纳米材料的形貌、成分及结构[11]。随后，采用图形化技术（如丝网印刷、喷墨打印等）将所得纳米材料进行组装/结构化[12]。此外，还需要后处理工艺对结构性能进一步调控（如热退火、热烧结等）。分步制造需要多种技术的配合，增加了工艺成本且过程复杂。因此，开发低成本微纳结构的制造技术是近年来研究的热门课题之一。

激光加工利用激光束与材料相互作用时产生的加热、熔化、汽化、形成等离子体、烧蚀等效应来完成[13]。作为近年飞速发展起来的先进加工技术，激光加工为微/纳米结构制造提供了新途径[14-15]。目前，激光加工已被广泛应用于各种微纳材料的制造，如贵金属、金属氧化物、碳系材料（如石墨烯和氧化石墨烯）等[13,16-20]。本文从“自下而上”的微纳结构激光加工方法入手，列举了激光组装、激光烧结/连接、激光合成及结构化在微/纳米结构制备中的应用，并与其他制造方法进行了对比。重点讨论了基

收稿日期：2020-11-23；**修回日期**：2020-12-21；**录用日期**：2021-02-23

基金项目：国家重点研发计划（2017YFB1104900）、国家自然科学基金（51975033）、北京市自然科学基金（3192020）

* **E-mail**：ppeng@buaa.edu.cn

于铜离子前驱体的激光直写方法，详细论述了前驱体成分/状态以及激光工艺参数对铜基结构的组织、成分、电学性能的影响。分析了激光直写铜微纳结构性能的调控方法，并针对其工艺难点、应用方向、发展趋势进行了展望。

2　“自下而上”的微纳结构激光加工

可利用激光将分散于溶液中的预合成纳米粒子在目标基板上进行组装/图形化。相较于常用的喷墨打印技术[12]，非接触式激光组装/图案化避免了诸如喷头堵塞、喷头污染带来的加工系统损耗，减小了其对结构化质量的影响。如图 1(a)所示，激光所引起的局部温度梯度将在溶液中引起热对流，将纳米颗粒牵引至光斑焦点附近，并通过范德瓦耳斯力在固-液界面组装[21]。组装过程中的温度梯度主要由激光辐照目标材料所产生的表面等离子体共振(SPR)引起，不同形貌/种类纳米材料的共振波长并不一致，因此选择相应波长的激光是成功组装纳米结构的关键。例如，金纳米颗粒的共振波长约 530 nm，采用 532 nm 波长的激光进行辐照具有较高的组装效率；而对于金纳米棒而言，785 nm 波长的激光是更好的选择[21]。通过改变激光的焦点位置，可在指定区域固定纳米结构。另外，也可利用激光辐照所产生的微气泡对纳米材料进行捕获[22-23]。光诱导微气泡与溶液的界面将形成 Marangoni 流体，所引起的牵引力将在气泡周围组装纳米结构[24]。纳米结构的形状及尺寸可以通过微泡大小来进行调控：当微泡尺寸显著大于纳米颗粒尺寸时，将形成空心的半球形三维结构；当微泡尺寸与纳米颗粒相当时，将形成二维环状结构[25]。进一步来讲，可以通过操控激光的行进路径来移动微泡，完成连续结构的图形化设计[26]。该过程中，微泡的稳定性是成功组装纳米材料的关键因素，可通过调整激光的脉冲宽度/频率来维持。

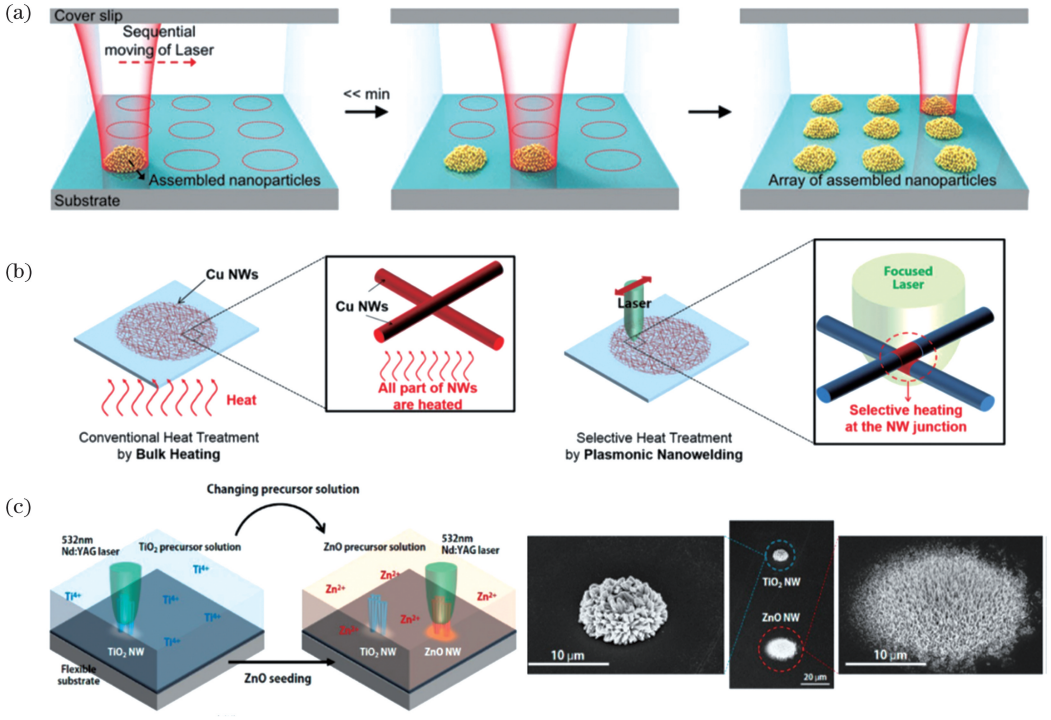

图 1　典型微纳结构的“自下而上”激光加工。(a)光诱导组装[21]；(b)激光烧结(与炉中烧结对比)[27]；(c)光诱导水热法合成[28]

Fig. 1　Typical “bottom-up” laser processing of micro/nano structures. (a) Laser-induced assembly[21]; (b) comparison of laser sintering and bulk heating[27]; (c) laser-induced hydrothermal growth[28]

除通过分子间作用力完成纳米材料组装外，可通过激光辐照完成纳米材料的连接/烧结。传统的炉中烧结技术需要整体升温，通常需要在高温下进行(>300 ℃)，不仅耗时且易造成柔性基板烧损[6]。如图 1(b)所示，激光烧结将高度集中的能量控制在所需区域，避免了长时间、大面积加热对基板的损害。在激光辐照纳米材料时，不仅通过光-热作用使材料局部升温，而且辐照所引起的 SPR 效应亦可促进纳米材料表面的熔化并完成连接[27,29-30]。这种低热作用下局部能量的累积可进一步降低宏观温升。

此外，激光烧结通过对材料连接及结构化的整合，相较于其他光子烧结方法（如强光烧结[31]），具有无掩模直接加工的能力。

激光不仅可加工预合成纳米材料，且可基于离子态前驱体完成纳米材料的合成。与水热法类似，激光合成纳米材料亦可通过氧化还原反应进行。如图 1(c)所示，激光辐照液态前驱体时，将在液体与基板的固-液界面处引起温升，诱导前驱体溶液局部区域发生化学反应，完成所需纳米结构的合成[32]。由于液态前驱体方便移除，可通过前驱体的更换，在同一基板上获得不同的纳米结构。在该过程中，可通过调整激光工艺参数、前驱体成分、基板属性对纳米结构进行控制。例如：可采用高透光率/低热导率的基板吸收层获得尺寸更精细的纳米线团簇[28]；可通过对辐照激光的输出形式（脉冲/连续）完成纳米线或块体结构的制备[33]。通过激光辐照干燥后的前驱体，可以完成纳米材料的合成。调控激光的行进路径同样可完成微纳结构的图形化[34-37]。通过激光与材料的交互作用完成加工，并将其进一步图形化的过程，可认为是广义上的激光直写。

3　激光直写铜基微纳结构及其电性能调控

3.1　激光直写导电铜结构工艺

基于预合成的铜纳米材料，可利用激光直写完成其连接及图形化。由于快速、低热作用的工艺特点，铜纳米材料的激光烧结无需额外的保护气氛/真空环境[38]。由于不同类型的激光具有不同的加工特性，选择合适的激光类型（尤其是激光波长）有利于抑制铜纳米材料在烧结时的氧化。例如，光诱导的 SPR 效应仅会在纳米结构的结节处引起局部温升形成连接，可有效避免整体加热引起的铜结构氧化。对于薄层（数纳米至数十纳米）铜纳米线的烧结而言，532 nm 波长的激光（对应铜纳米线共振波长）是较优选择[27]；由于激光的穿透深度与其波长正相关，对于厚层（数百纳米至微米级）纳米铜结构的烧结，近红外波长的激光更具优势：采用 1064 nm 波长的激光烧结铜纳米颗粒时，热量将主要向深度方向传导，仅表面与空气接触的铜纳米材料发生少量氧化[29]。但预合成的铜纳米材料容易在储存过程中氧化，导致烧结所需的能量升高，最终结构的导电性降低[39]。因此采用激光烧结铜材料前，需要额外的预处理步骤去除氧化物薄膜[40]。为克服这一问题，可采用具有更低成本、更易保存的铜氧化物作为前驱体[41]。在铜氧化物（氧化铜或氧化亚铜）中加入还原剂后，可利用激光直写将铜氧化物还原为铜纳米材料，并进一步完成其烧结。一方面，激光通过热作用分解还原剂，完成铜纳米材料的还原。另一方面，激光辐照铜氧化物引起的电子跃迁也将促进其还原[42]。激光热效应与波长正相关，但光子能量与波长成反比。光诱导电子跃迁需要光子能量高于氧化物的带隙，由于氧化铜的带隙（约 1.2 eV）低于氧化亚铜（约 2.1 eV）[43]，故氧化铜可匹配更长波长的激光（兼具光-热作用及光致电子跃迁作用），更适合作为前驱体使用。但该还原-烧结进程仍是基于预合成材料。从工艺流程简化及成本节约的角度出发，基于离子态前驱体的激光直写一步法被认为是更加高效的铜微纳结构制造技术。离子态前驱体由铜盐及还原剂组成，激光辐照将诱导其中还原剂分解并合成铜纳米结构，同时将其原位连接为导电结构[44-45]。基于离子态前驱体的激光直写不仅可规避预合成铜纳米材料的氧化问题，且将铜纳米材料的合成、烧结及结构化整合为一个步骤，极大地提高了铜微纳结构的制造效率。

图 2 示出了激光直写离子态铜盐前驱体的典型工艺流程。其中，离子态前驱体通常由铜盐及还原剂的简单溶解/混合获得。在通过滴涂/旋涂/棒涂等方法将前驱体溶液置于目标基板后，可采用低温加热对离子态前驱体进行烘干以获得均匀的前驱体薄膜。该技术适用于包含热敏基板在内的各种基板，如玻璃[46]、聚对苯二甲酸乙二醇酯[44]、聚酰亚胺[47]及聚碳酸酯[48]等。随后利用聚焦激光束对所需区域进行辐照，完成铜微/纳结构的合成及烧结。多种激光光源，如 CO_2 激光[49]、半导体激光[45]、飞秒激光[50]均可用于铜微纳结构的直写。通过控制行进激光的扫描路径，可在无模板的条件下完成各种复杂图案的定制（即激光图案化）。完成图案化后，清洗去除未辐照的前驱体，即可获得所设计的铜微/纳结构。在该过程中，前驱体成分及激光工艺参数是影响铜微纳结构组织及性能的重要因素。

还原剂是成功合成铜微纳结构的关键。具有羟基（—OH 基团）的醇/多元醇，如甲醇、乙醇、异丙醇等均可用于铜纳米材料的合成[43]。其中，乙二醇因其沸点高、蒸发速率慢等特点被认为是较优的还原剂[43]。一般来讲，多元醇通过分解形成的醛基起到了还原作用[51]：

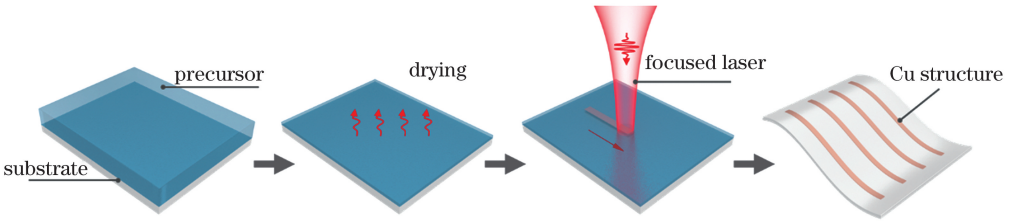

图 2　基于离子态铜盐前驱体的激光直写典型工艺流程

Fig. 2　Typical manufacturing process of the direct laser writing based on the copper ionic precursor

$$2HO(CH_2)_2 \xrightarrow{\Delta(heat)-2H_2O} 2C_2H_4O \xrightarrow{Cu(Ⅱ)} C_4H_6O_2+H_2O+Cu。 \tag{1}$$

含羧基(—COOH 基团)的有机物及无机物[例如聚乙烯吡咯烷酮(PVP)、乙酸(CH_3COOH)、甲酸(HCOOH)]也可用于铜纳米材料的还原[49]。以 PVP 为例，激光热作用将 PVP 分解为亚甲基结构、甲胺和丙酸。丙酸将进一步分解成甲酸并将 Cu^{2+} 还原为 Cu^0[45, 52]：

$$2CuO+HCOOH \xrightarrow{\Delta(heat)-2H_2O} Cu_2O+CO_2+HCOOH \xrightarrow{\Delta(heat)-2H_2O} 2Cu+CO_2。 \tag{2}$$

值得注意的是，激光诱导的还原/合成过程很大程度上取决于氧化还原的反应温度。这意味着虽然激光可将升温区域局限在非常小的区域内，但仍然需要达到对应的温度阈值。例如多元醇的分解温度在 180 ℃左右[43]，而甲酸约为 100 ℃[53]。由于含羧基还原剂的分解温度更低，含羧基还原剂将比多元醇更适用于在热敏基板上直写导电铜结构。

激光工艺参数是影响直写结构特征尺寸、成分及微观组织的重要因素。激光的光斑直径决定了直写铜结构的线宽。由于大多激光的光束能量为高斯分布，其中心区域的热输入要高于边缘[19,48]。如图 3(a)所示，当能量输入较低时，仅有辐照的中心区域达到了反应的温度阈值，所得结构的线宽略低于所采用的光斑直径(区域Ⅰ)。增加能量输入将宽化反应区域，且水平方向的热扩散将一定程度引起辐照区域外侧的温升(区域Ⅱ，热影响区)，导致所得结构的线宽大于光斑直径。足够的能量输入是确保铜充分还原、保证结构导电性的关键因素。当采用较低功率进行直写时，所得结构表面呈现出灰暗的铜氧化物色泽，而高功率下获得结构表面则展现出

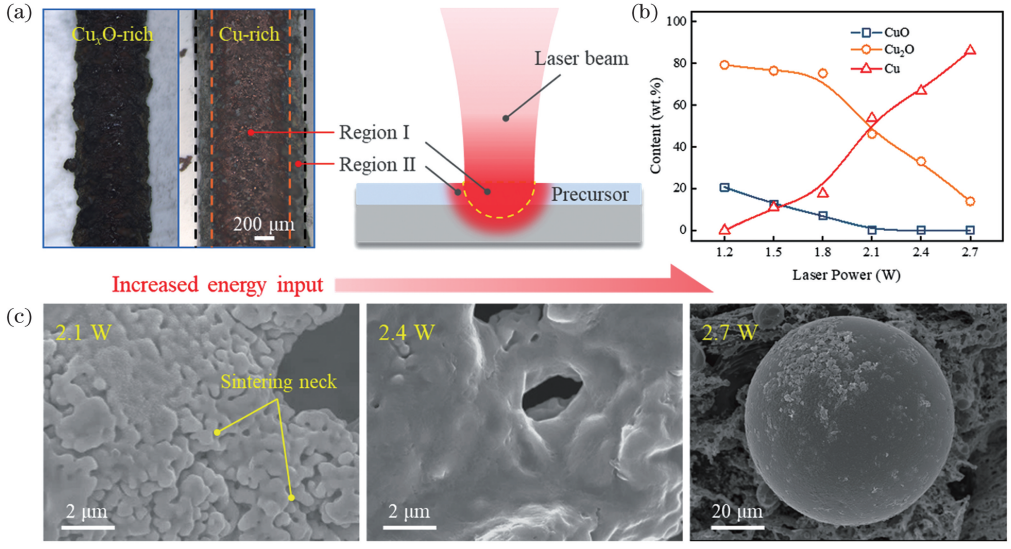

图 3　激光工艺参数对直写铜结构的影响[48]。(a)线宽；(b)成分；(c)微观组织

Fig. 3　Effect of laser parameters on the written copper structure[48]. (a) Width of structure; (b) composition; (c) microstructure

铜的金属光泽。这是由于当激光功率较低时，所提供的能量不足以完全分解还原剂，结构的主要成分为铜氧化物。随着激光功率的增加，铜氧化物减少而铜含量逐渐升高[如图 3(b)所示]。所合成的铜纳米颗粒将在激光的作用下发生连接。如图 3(c)所示，低功率激光直写时在获得的结构中可以观察到烧结颈。升高激光功率将增强所引起的热效应/等离子激元效应，颗粒间的烧结颈逐渐长大并形成连续结构。但进一步增加输入能量将使纳米颗粒完全熔化，破坏结构连续性，降低其导电性[54]。此外，在对干燥后的离子态前驱体激光直写时，前驱体中还原剂等物质的挥发和气化容易在所得结构中形成孔洞[42]。虽可通过激光工艺调控来降低孔隙率，但很难完全避免。基于液态前驱体的激光直写有望改善所得结构的致密程度[47]。在直写液态铜离子前驱体时，虽溶剂等配体蒸发将引入孔洞，但在单次激光扫描后液体将会重新回填。在同一轨迹处增加扫描次数时，将形成新的纳米结构填补孔隙，进而获得致密的直写结构。

3.2　激光直写铜基微纳结构的电性能及其调控

对于铜导电结构而言，导电性是其性能评价的重要指标之一。在获得高铜含量的导电结构后，其导电性能主要受到孔隙率的影响。图 4 列出了目前基于不同前驱体(铜纳米颗粒[29,38,55]、铜氧化物颗粒[41-42]、固/液态离子前驱体[44-45,47,56-58])所获得的典型铜导电结构的电阻率，其中插图绘制了相对应结构的典型微观形貌。可以看出，铜结构的导电性与其致密程度正相关。基于氧化铜纳米颗粒及干燥状态的铜离子前驱体所获的铜结构电阻率通常为 $10\sim10^3$ μΩ·cm，较铜块材电阻率高出 1～2 个数量级。而基于预合成铜纳米颗粒及液态铜离子前驱体所获的直写结构具有更低的孔隙率，其电阻率的数量级与块材相当(≤10 μΩ·cm)。

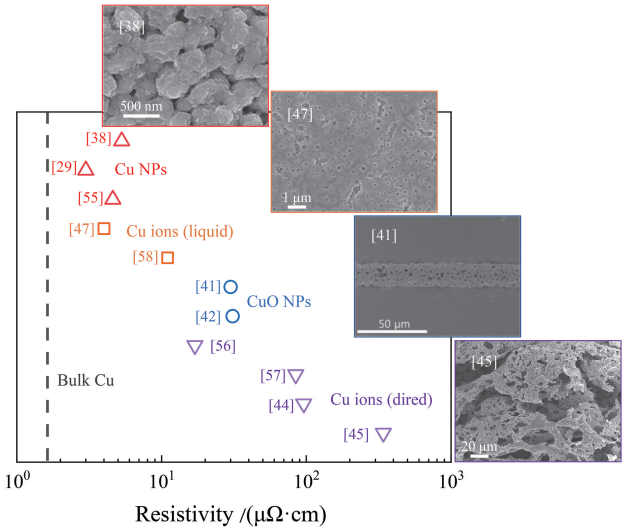

图 4　基于不同前驱体直写所得典型铜微结构的电阻率及微观形貌比较

Fig. 4　Comparison of resistivity and microstructure of the laser written copper structures based on different precursors

对于导电铜微纳米结构而言，其氧化问题不仅存在于储存及加工过程中，服役过程中结构的氧化也将导致其导电性能损失[59]。在完成导电铜结构的制备后，通常利用封装层[如聚二甲基硅氧烷(PDMS)[44]、聚甲基丙烯酸甲酯(PMMA)[60]等]来隔绝空气，避免结构氧化。显然额外的封装工艺将使导电结构的制造过程复杂化，提高了成本。制备铜基核壳结构(如铜@银[61-63]、铜@金-银合金[64]、铜@镍[65]、铜@石墨烯[66]等)是提高结构稳定性的有效手段。通过对激光直写所用前驱体成分的调控，可完成复合结构的制备。如图 5(a)所示，当采用 PVP 还原铜结构时，PVP 的分解将引入无定形碳，在激光的热作用下，无定形碳将被部分晶化为石墨，形成独特的铜碳复合结构[45]。类似地，可以有意地在前驱体中引入额外的有机物作为碳源。如图 5(b)所示，通过在前驱体中添加鞣酸作为碳源，也可获得铜碳包覆结构[47]。相较于高温化学沉积(CVD)技术[67-70]，激光直写过程的温度较低，因而结构中获得的碳结构主要为非晶碳。此外，在引入碳结构后，由于碳-铜间仅有范德瓦耳斯力，并未形成冶金结合，故直写结构的孔隙率将有所升高，略微地降低了其导电性，但碳对铜的包覆作用将显著提高直写结构在服役过程中的抗氧化性能。如图 5(c)所示，所得结构在近 100 ℃下存放于大气中后，其电阻仍然保持恒定，而铜结构已经因氧化而导致相对电阻上升。

此外，虽对于导电铜基结构而言，氧化物是不期望的缺陷，但对于功能结构而言，铜氧化物具有半导体的特点，具有开发为功能结构的潜力。激光直写为功能结构及导电结构的可控制备提供了新思路。如图 5(d)所示，低激光能量输入的情况下，直写结构的表面存在着大量氧化物纳米片[48]。所得的氧化铜与氧化亚铜在激光作用下发生连接，故图中可以观察到明显的连接界面。由于激光功率较低，氧化物维持在纳米尺度，保留了高比表面积的特性。此外，采用过量的能量输入或低扫描速度激光直写时，所还原的铜结构将在大气环境中被再次氧化，同样可获得富氧化物结构[49]。由于高能量输入下的激光烧结作用，所得氧化物通常在微米级。

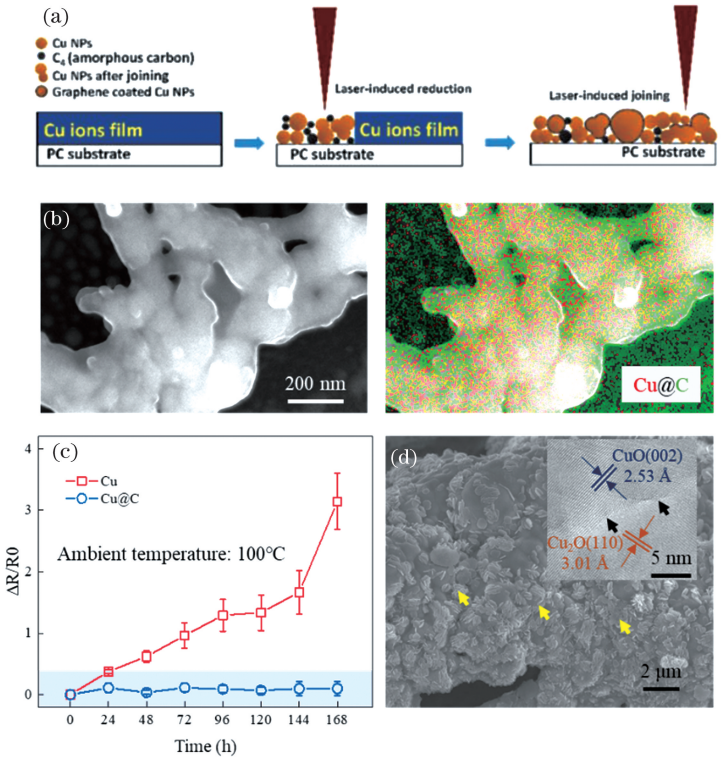

图 5　激光直写铜基复合微纳结构。(a)铜碳复合结构的形成机理示意[45]；(b)典型铜碳复合结构的微观形貌及元素分布；(c)铜碳复合结构与铜结构的抗氧化性能比较[47]；(d)低激光功率下直写铜氧化物的结构[48]

Fig. 5　Direct laser writing of Cu-based composite micro-nano structure. (a) Schematic diagram of the formation mechanism of the Cu-C composite structure[45]; (b) microstructure and elements distribution of the typical Cu-C composite structure; (c) comparison of oxidation resistance of Cu and Cu-C structures[47]; (d) structure of the directly written Cu oxides at a low laser power[48]

4　直写铜微纳结构的典型应用

4.1　导电铜结构的应用

导电电极是激光直写铜微纳结构的典型应用之一。如图 6(a)所示，直写在柔性基板上的铜电极可以在弯曲状态下工作[47]。除此之外，图案化后的导电铜结构与其他功能组件配合可实现更多的功能性器件设计。如图 6(b)所示，可将铜微结构转印至 PDMS 上完成应变传感器的制造。将器件固定于手指后，手指弯曲会引起铜结构电阻上升，手指恢复平直状态后，结构的电阻也将随之恢复，从而达到监控手指运动的目的。如图 6(c)所示，通过直写铜导电结构，并与介电层配合，可完成多点式接近/触摸传感器的制造[71]。导电结构与介电层组装的叠层结构，能够在很宽的范围内感应出很强的边缘场，移动导电物体会引起该边缘场的干扰，从而导致其电容发生变化[72-73]。可以通过监视顶部和底部电极层之间的互电容来检测传感元件附近导电物体的相对位置。如图 6(d)所示，可将导电铜微结构图形化为平面天线，与商用 IC 芯片配合完成诸如近场通信(NFC)、射频识别(RFID)及无线充电设备的制造[45, 74-75]。对于该类器件，结构的导电性是其性能的重要决定因素之一，高电导率有利于减少电路内耗，降低器件操作电压；可提高接近传感器的监测距离[71]；可提高所制备天线的效率及(有效)增益[76]等。

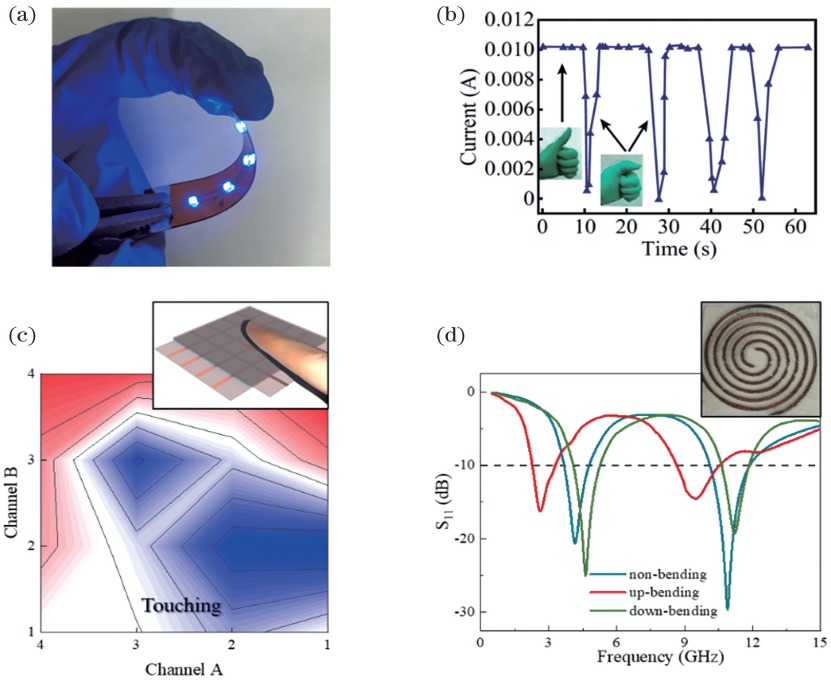

图 6　导电铜结构的典型应用。(a)柔性电极[47]；(b)应变传感器对手指运动的监测[44]；(c)接近/触摸传感器对手指触摸的响应[71]；(d)柔性平面天线及其频宽[45]

Fig. 6　Typical applications of the conductive Cu structures. (a) Flexible electrode[47]; (b) monitoring the finger movement using the strain sensor[44]; (c) response of the proximity/touch sensor to finger touch[71]; (d) planar antenna and its bandwidth[45]

4.2　功能性铜基结构的应用

激光直写制备的复合结构可以拓宽铜基结构的应用范围。当在闭合导电通路两端施加电压时，结构将在焦耳热效应的作用下升温。如图7(a)所示，

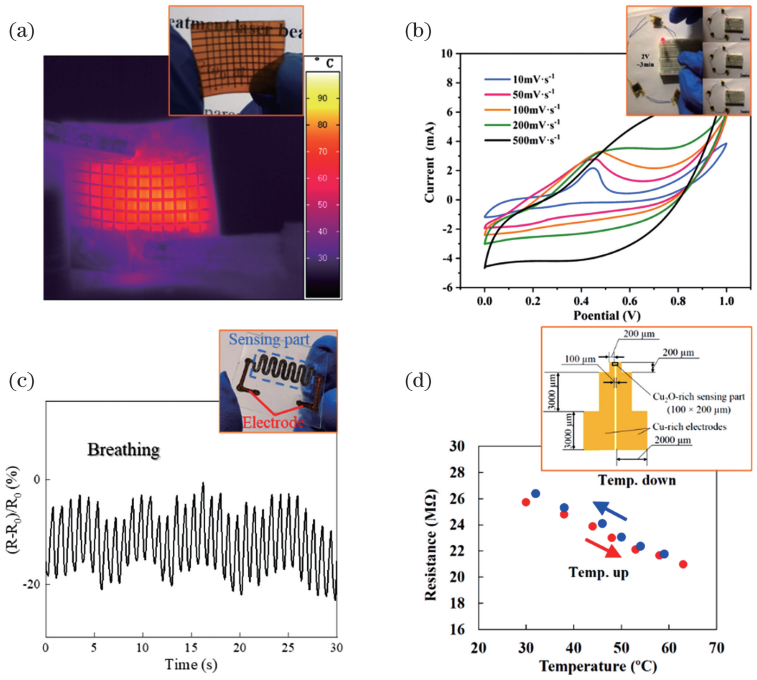

图 7　激光直写功能性铜基结构的典型应用。(a)柔性加热器[47]；(b)准固态电容器及其循环伏安曲线[46]；(c)湿度传感器对呼吸频率的监测[48]；(d)温度传感器及其温度响应曲线[84]

Fig. 7　Typical applications of the laser written functional Cu-based structures. (a) Flexible heater[47]; (b) quasi-solid capacitor and its cyclic voltammogram[46]; (c) monitoring the breath rate using the strain sensor[48]; (d) temperature sensor and its temperature response curves[84]

利用铜碳结构良好的抗氧化性能，可在无需封装的情况下完成柔性加热器的制造[47]。铜在电化学过程中将发生可逆的氧化还原反应，展现出赝电容的特性[77]；而碳结构具有双电层电容的特点[78]。如图 7(b)所示，基于铜碳复合材料可以完成准固态电容器的开发，独特的复合结构使得器件较碳基电容器具有更高的比电容[46]。铜氧化物感测结构置于空气中时，其表面电子将被吸附氧俘获，形成空穴累积层。当环境状态如特种气体[79]、湿度[80]、光子强度[81]等发生变化时，将引起纳米材料的表面耗尽层厚度改变，导致电信号变化。利用激光直写对结构的可调控性，可以一步制造包含功能结构(富铜氧化物结构)和导电电极(富铜结构)的集成器件。如图 7(c)所示，采用低能量输入下获得的富氧化物作为湿度传感部件，通过直写富铜结构作为电极，可制造集成化湿度传感器[48]。当人体呼吸造成环境湿度变化时，水分子首先在纳米材料表面发生电离，其解离的 H^+ 与纳米材料表面吸附的双离子氧化反应形成 OH^-，从而释放出捕获的电子并中和空穴[82]。所引起的电信号变化将由导电电极导出，完成了对呼吸频率的监测。类似地，如图 7(d)所示，分别采用高/低扫描速度完成富铜结构及富氧化亚铜结构的制造，进一步完成集成化温度传感器的开发[83-84]。

5　结束语

总而言之，由于其无接触、无需掩模及加工快速的特点，激光直写已成为铜微纳结构的高效制造技术。基于离子态前驱体的激光直写整合了铜纳米材料的合成、定位、组装及连接，且在结构及成分的调控方面展现出独特的优势。目前，已掌握了在多种类型基板上可控直写铜基微纳结构的方法，且据此开发了多种微电子器件原型。应该指出的是，激光直写铜微纳结构仍然存在着亟待解决的问题：目前激光直写铜结构的研究主要仍针对纯铜结构展开，复合结构的制造方法尚不成熟；相较于分步制造方法，激光直写对铜材料的纳观结构(例如尺寸、均匀性)很难控制；虽可通过激光参数的调控对结构的成分(铜及铜氧化物)进行一定程度的调控，但所获铜结构通常为多组分复合结构。此外，一步法激光直写过程涉及到包含物理化学在内的多学科交叉，其直写机理尚未完全明确：如采用不同波长/类型激光直写所得结构的特征(成分、连接程度等)有待对比；直写过程中不同程度的热/等离子激元效应对所得铜结构的影响有待明确；直写过程中复合材料的还原、连接机理尚需深入研究；基于液态前驱体直写过程中流体的影响有待明晰。激光直写机理、直写结构的精细调控及复合铜基结构的制备将是未来相关研究开展的重要命题。再者，激光直写所得铜基结构的应用范围尚有扩展空间，直写结构的组织、成分及电性能对器件性能的影响尚待阐明，且器件的性能有待进一步优化。

参　考　文　献

[1] Wang X D, Dong L, Zhang H L, et al. Recent progress in electronic skin[J]. Advanced Science, 2015, 2(10): 1500169.

[2] Nathan A, Ahnood A, Cole M T, et al. Flexible electronics: the next ubiquitous platform[J]. Proceedings of the IEEE, 2012, 100: 1486-1517.

[3] Kim J, Kim M, Lee M S, et al. Wearable smart sensor systems integrated on soft contact lenses for wireless ocular diagnostics[J]. Nature Communications, 2017, 8: 14997.

[4] Kim K K, Ha I, Won P, et al. Transparent wearable three-dimensional touch by self-generated multiscale structure[J]. Nature Communications, 2019, 10: 2582.

[5] Peng P, Hu A, Gerlich A P, et al. Joining of silver nanomaterials at low temperatures: processes, properties, and applications[J]. ACS Applied Materials & Interfaces, 2015, 7(23): 12597-12618.

[6] Kamyshny A, Magdassi S. Conductive nanomaterials for 2D and 3D printed flexible electronics[J]. Chemical Society Reviews, 2019, 48(6): 1712-1740.

[7] Li W L, Sun Q Q, Li L Y, et al. The rise of conductive copper inks: challenges and perspectives[J]. Applied Materials Today, 2020, 18: 100451.

[8] Sun S D, Zhang X J, Yang Q, et al. Cuprous oxide (Cu_2O) crystals with tailored architectures: a comprehensive review on synthesis, fundamental properties, functional modifications and applications[J]. Progress in Materials Science, 2018, 96: 111-173.

[9] Zhang Q B, Zhang K L, Xu D G, et al. CuO nanostructures: synthesis, characterization, growth mechanisms, fundamental properties, and applications[J]. Progress in Materials Science, 2014, 60: 208-337.

[10] Sun S. Recent advances in hybrid Cu_2O-based heterogeneous nanostructures[J]. Nanoscale, 2015, 7(25): 10850-10882.

[11] Bhanushali S, Ghosh P, Ganesh A, et al. 1D copper nanostructures: progress, challenges and opportunities[J]. Small, 2015, 11(11): 1232-1252.

[12] Choi Y, Seong K D, Piao Y Z, et al. Metal: organic decomposition ink for printed electronics [J]. Advanced Materials Interfaces, 2019, 6(20): 1901002.

[13] Palneedi H, Park J H, Maurya D, et al. Laser processing of metal oxides: laser irradiation of metal oxide films and nanostructures: applications and advances [J]. Advanced Materials, 2018, 30(14): 1870094.

[14] Gao S H, Yu X Y, Song X, et al. Compart mentalized out-of-plane alignment of liquid crystals based on femtosecond laser direct writing and its applications[J]. Chinese Journal of Lasers, 2019, 46(5): 0508009.
高少华, 禹宣伊, 宋筱, 等. 基于飞秒激光直写的液晶面外区域定向技术及其应用[J]. 中国激光, 2019, 46(5): 0508009.

[15] Shi Y, Xu B, Wu D, et al. Research progress on fabrication of functional microfluidic chips using femtosecond laser direct writing technology [J]. Chinese Journal of Lasers, 2019, 46(10): 1000001.
史杨, 许兵, 吴东, 等. 飞秒激光直写技术制备功能化微流控芯片研究进展[J]. 中国激光, 2019, 46(10): 1000001.

[16] Zhao C L, Shah P J, Bissell L J, et al. Laser additive nano-manufacturing under ambient conditions [J]. Nanoscale, 2019, 11(35): 16187-16199.

[17] Kumar R, Singh R K, Singh D P, et al. Laser-assisted synthesis, reduction and micro-patterning of graphene: recent progress and applications [J]. Coordination Chemistry Reviews, 2017, 342: 34-79.

[18] Joe D J, Kim S, Park J H, et al. Laser-material interactions for flexible applications [J]. Advanced Materials, 2017, 29(26): 1606586.

[19] Chen Z Y, Fang G, Cao L C, et al. Direct writing of silver micro-nanostructures by femtosecond laser tweezer[J]. Chinese Journal of Lasers, 2018, 45(4): 0402006.
陈忠赟, 方淦, 曹良成, 等. 飞秒激光光镊直写银微纳结构[J]. 中国激光, 2018, 45(4): 0402006.

[20] Huang Y X, Chen X P, Yu J B, et al. Graphene-based film heater fabricated by laser writing [J]. Materials Letters, 2021, 284: 128869.

[21] Jin C M, Lee W, Kim D, et al. Photothermal convection lithography for rapid and direct assembly of colloidal plasmonic nanoparticles on generic substrates[J]. Small, 2018, 14(45): e1803055.

[22] Rajeeva B B, Wu Z L, Briggs A, et al. Direct-write printing: "point-and-shoot" synthesis of metallic ring arrays and surface-enhanced optical spectroscopy [J]. Advanced Optical Materials, 2018, 6(10): 1870038.

[23] Yamamoto Y, Tokonami S, Iida T, et al. Surfactant-controlled photothermal assembly of nanoparticles and microparticles for rapid concentration measurement of microbes [J]. ACS Applied Bio Materials, 2019, 2(4): 1561-1568.

[24] Lü C J, Varanakkottu S N, Baier T, et al. Controlling the trajectories of nano/micro particles using light-actuated Marangoni flow [J]. Nano Letters, 2018, 18(11): 6924-6930.

[25] Lin L H, Peng X L, Mao Z M, et al. Bubble-pen lithography [J]. Nano Letters, 2016, 16(1): 701-708.

[26] Armon N, Greenberg E, Layani M, et al. Continuous nanoparticle assembly by a modulated photo-induced microbubble for fabrication of micrometric conductive patterns [J]. ACS Applied Materials & Interfaces, 2017, 9(50): 44214-44221.

[27] Han S, Hong S, Ham J, et al. Fast plasmonic laser nanowelding for a Cu-nanowire percolation network for flexible transparent conductors and stretchable electronics[J]. Advanced Materials (Deerfield Beach, Fla.), 2014, 26(33): 5808-5814.

[28] Yeo J, Hong S, Kim G, et al. Laser-induced hydrothermal growth of heterogeneous metal-oxide nanowire on flexible substrate by laser absorption layer design [J]. ACS Nano, 2015, 9(6): 6059-6068.

[29] Park J H, Jeong S, Lee E J, et al. Transversally extended laser plasmonic welding for oxidation-free copper fabrication toward high-fidelity optoelectronics [J]. Chemistry of Materials, 2016, 28(12): 4151-4159.

[30] Lee C, Hahn J W. Calculating the threshold energy of the pulsed laser sintering of silver and copper nanoparticles [J]. Journal of the Optical Society of Korea, 2016, 20(5): 601-606.

[31] Park J H, Han S, Kim D, et al. Plasmonic-tuned flash Cu nanowelding with ultrafast photochemical-reducing and interlocking on flexible plastics [J]. Advanced Functional Materials, 2017, 27(29): 1701138.

[32] Yeo J, Hong S, Wanit M, et al. Rapid, one-step, digital selective growth of ZnO nanowires on 3D structures using laser induced hydrothermal growth [J]. Advanced Functional Materials, 2013, 23(26): 3316-3323.

[33] Kwon K, Shim J, Lee J O, et al. Localized laser-based photohydrothermal synthesis of functionalized metal-oxides [J]. Advanced Functional Materials, 2015, 25(15): 2222-2229.

[34] Fujii S, Fukano R, Hayami Y, et al. Simultaneous

formation and spatial patterning of ZnO on ITO surfaces by local laser-induced generation of microbubbles in aqueous solutions of $[Zn(NH_3)_4]^{2}$ [J]. ACS Applied Materials & Interfaces, 2017, 9(9): 8413-8419.

[35] Ren X L, Zheng M L, Jin F, et al. Laser direct writing of silver nanowire with amino acids-assisted multiphoton photoreduction [J]. The Journal of Physical Chemistry C, 2016, 120(46): 26532-26538.

[36] Liu Y K, Lee M T. Laser direct synthesis and patterning of silver nano/microstructures on a polymer substrate [J]. ACS Applied Materials & Interfaces, 2014, 6(16): 14576-14582.

[37] Yu S Y, Schrodj G, Mougin K, et al. Direct laser writing of crystallized TiO_2 and TiO_2/carbon microstructures with tunable conductive properties [J]. Advanced Materials, 2018, 30(51): e1805093.

[38] Yu J H, Kang K T, Hwang J Y, et al. Rapid sintering of copper nano ink using a laser in air[J]. International Journal of Precision Engineering and Manufacturing, 2014, 15(6): 1051-1054.

[39] Jeong S, Woo K, Kim D, et al. Controlling the thickness of the surface oxide layer on Cu nanoparticles for the fabrication of conductive structures by ink-jet printing [J]. Advanced Functional Materials, 2008, 18(5): 679-686.

[40] Kwon J, Cho H, Suh Y D, et al. Flexible and transparent Cu electronics by low-temperature acid-assisted laser processing of Cu nanoparticles [J]. Advanced Materials Technologies, 2017, 2(2): 1600222.

[41] Kang B, Han S, Kim J, et al. One-step fabrication of copper electrode by laser-induced direct local reduction and agglomeration of copper oxide nanoparticle[J]. The Journal of Physical Chemistry C, 2011, 115(48): 23664-23670.

[42] Back S, Kang B. Low-cost optical fabrication of flexible copper electrode via laser-induced reductive sintering and adhesive transfer[J]. Optics and Lasers in Engineering, 2018, 101: 78-84.

[43] Han S, Hong S, Yeo J, et al. Nanorecycling: monolithic integration of copper and copper oxide nanowire network electrode through selective reversible photothermochemical reduction [J]. Advanced Materials, 2015, 27(41): 6397-6403.

[44] Bai S, Zhang S G, Zhou W P, et al. Laser-assisted reduction of highly conductive circuits based on copper nitrate for flexible printed sensors[J]. Nano-Micro Letters, 2017, 9(4): 1-13.

[45] Peng P, Li L H, He P, et al. One-step selective laser patterning of copper/graphene flexible electrodes [J]. Nanotechnology, 2019, 30(18): 185301.

[46] Liao J, Guo W, Peng P. Direct laser writing of copper-graphene composites for flexible electronics [J]. Optics and Lasers in Engineering, 2021, 142: 106605.

[47] Zhou X W, Guo W, Zhu Y, et al. The laser writing of highly conductive and anti-oxidative copper structures in liquid [J]. Nanoscale, 2020, 12(2): 563-571.

[48] Zhou X W, Guo W, Fu J, et al. Laser writing of Cu/Cu_xO integrated structure on flexible substrate for humidity sensing[J]. Applied Surface Science, 2019, 494: 684-690.

[49] Mizoshiri M, Aoyama K, Uetsuki A, et al. Direct writing of copper micropatterns using near-infrared femtosecond laser-pulse-induced reduction of glyoxylic acid copper complex[J]. Micromachines, 2019, 10(6): 401.

[50] Liao J N, Wang X D, Zhou X W, et al. Femtosecond laser direct writing of copper microelectrodes [J]. Chinese Journal of Lasers, 2019, 46(10): 1002013.
廖嘉宁, 王欣达, 周兴汶, 等. 飞秒激光直写铜微电极研究[J]. 中国激光, 2019, 46(10): 1002013.

[51] Zarzar L D, Swartzentruber B S, Donovan B F, et al. Usinglaser-induced thermal voxels to pattern diverse materials at the solid-liquid interface [J]. ACS Applied Materials & Interfaces, 2016, 8(33): 21134-21139.

[52] Ryu J, Kim H S, Hahn H T, et al. Reactive sintering of copper nanoparticles using intense pulsed light for printed electronics[J]. Journal of Electronic Materials, 2011, 40(1): 42-50.

[53] Wang N, Liu Y, Guo W, et al. Low-temperature sintering of silver patterns on polyimide substrate printed with particle-free ink [J]. Nanotechnology, 2020, 31(30): 305301.

[54] Noh J, Ha J, Kim D, et al. Femtosecond and nanosecond laser sintering of silver nanoparticles on a flexible substrate[J]. Applied Surface Science, 2020, 511: 145574.

[55] Zenou M, Ermak O, Saar A, et al. Laser sintering of copper nanoparticles [J]. Journal of Physics D: Applied Physics, 2014, 47(2): 025501.

[56] Lee J, Lee B, Jeong S, et al. Microstructure and electrical property of laser-sintered Cu complex ink [J]. Applied Surface Science, 2014, 307: 42-45.

[57] Min H, Lee B, Jeong S, et al. Fabrication of 10 μm-scale conductive Cu patterns by selective laser sintering of Cu complex ink [J]. Optics & Laser Technology, 2017, 88: 128-133.

[58] Zehnder S, Lorenz P, Ehrhardt M, et al. Laser-induced processes on the back side of dielectric surfaces using a $CuSO_4$-based absorber liquid[J]. Proceedings of SPIE, 2014, 8968: 896812.

[59] Li W L, Yang Y, Zhang B W, et al. Highly densified Cu wirings fabricated from air-stable Cu complex ink with high conductivity, enhanced oxidation resistance, and flexibility[J]. Advanced Materials Interfaces, 2018, 5(19): 1800798.

[60] Zhai H T, Wang R R, Wang X, et al. Transparent heaters based on highly stable Cu nanowire films[J]. Nano Research, 2016, 9(12): 3924-3936.

[61] Li W, Li C F, Lang F, et al. Self-catalyzed copper-silver complex inks for low-cost fabrication of highly oxidation-resistant and conductive copper-silver hybrid tracks at a low temperature below 100 ℃[J]. Nanoscale, 2018, 10(11): 5254-5263.

[62] Yim C, Sandwell A, Park S S, et al. Hybrid copper-silver conductive tracks for enhanced oxidation resistance under flash light sintering[J]. ACS Applied Materials & Interfaces, 2016, 8(34): 22369-22373.

[63] Li W, Hu D, Li L, et al. Printable and flexible copper-silver alloy electrodes with high conductivity and ultrahigh oxidation resistance[J]. ACS Applied Materials & Interfaces, 2017, 9(29): 24711-24721.

[64] Zhang H, Tian Y H, Wang S, et al. Highly stable flexible transparent electrode via rapid electrodeposition coating of Ag-Au alloy on copper nanowires for bifunctional electrochromic and supercapacitor device[J]. Chemical Engineering Journal, 2020, 399: 125075.

[65] Kim T G, Park H J, Woo K, et al. Enhanced oxidation-resistant Cu@Ni core-shell nanoparticles for printed flexible electrodes[J]. ACS Applied Materials & Interfaces, 2018, 10(1): 1059-1066.

[66] Ye D M, Li G Z, Wang G G, et al. One-pot synthesis of copper nanowire decorated by reduced graphene oxide with excellent oxidation resistance and stability[J]. Applied Surface Science, 2019, 467/468: 158-167.

[67] Tseng C A, Chen C C, Ulaganathan R K, et al. One-step synthesis of antioxidative graphene-wrapped copper nanoparticles on flexible substrates for electronic and electrocatalytic applications[J]. ACS Applied Materials & Interfaces, 2017, 9(30): 25067-25072.

[68] Xu Y T, Guo Y, Song L X, et al. Facile fabrication of reduced graphene oxide encapsulated copper spherical particles with 3D architecture and high oxidation resistance[J]. RSC Advances, 2014, 4(101): 58005-58010.

[69] Lee S, Hong J, Koo J H, et al. Synthesis of few-layered graphene nanoballs with copper cores using solid carbon source[J]. ACS Applied Materials & Interfaces, 2013, 5(7): 2432-2437.

[70] Choi D, Pyo Y, Jung S B, et al. Application of thetaguchi method to optimize graphene coatings on copper nanoparticles formed using a solid carbon source[J]. Materials Transactions, 2016, 57(7): 1177-1182.

[71] Li Y K, Zhou X W, Chen J L, et al. Laser-patterned copper electrodes for proximity and tactile sensors[J]. Advanced Materials Interfaces, 2020, 7(4): 1901845.

[72] Zhang C, Liu S Y, Huang X, et al. A stretchable dual-mode sensor array for multifunctional robotic electronic skin[J]. Nano Energy, 2019, 62: 164-170.

[73] Liu Y Q, Zhang Y L, Jiao Z Z, et al. Directly drawing high-performance capacitive sensors on copying tissues[J]. Nanoscale, 2018, 10(36): 17002-17006.

[74] Zhang J H, Feng J, Jia L Y, et al. Laser-induced selective metallization on polymer substrates using organocopper for portable electronics[J]. ACS Applied Materials & Interfaces, 2019, 11(14): 13714-13723.

[75] Rahimi R, Es-haghi S S, Chittiboyina S, et al. Laser-enabled processing of stretchable electronics on a hydrolytically degradable hydrogel[J]. Advanced Healthcare Materials, 2018, 7(16): 1800231.

[76] Khan Y, Thielens A, Muin S, et al. A new frontier of printed electronics: flexible hybrid electronics[J]. Advanced Materials, 2020, 32(15): e1905279.

[77] Xu P P, Liu J J, Liu T, et al. Preparation of binder-free CuO/Cu_2O/Cu composites: a novel electrode material for supercapacitor applications[J]. RSC Advances, 2016, 6(34): 28270-28278.

[78] Cai J G, Watanabe A, Lü C, et al. Laser direct writing of carbon/Au composite electrodes for high-performance micro-supercapacitors[J]. Proceedings of SPIE, 2017, 10092: 100920P.

[79] Tiemann M. Porous metal oxides as gas sensors[J]. Chemistry-A European Journal, 2007, 13(30): 8376-8388.

[80] Wang Z Y, Xiao Y, Cui X B, et al. Humidity-sensing properties of urchinlike CuO nanostructures modified by reduced graphene oxide[J]. ACS Applied Materials & Interfaces, 2014, 6(6): 3888-3895.

[81] Noothongkaew S, Thumthan O, An K S, et al. UV-Photodetectors based on CuO/ZnO nanocomposites

[J]. Materials Letters, 2018, 233: 318-323.

[82] Hsu C L, Tsai J Y, Hsueh T J, et al. Ethanol gas and humidity sensors of CuO/Cu_2O composite nanowires based on a Cu through-silicon via approach [J]. Sensors and Actuators B: Chemical, 2016, 224: 95-102.

[83] Arakane S, Mizoshiri M, Sakurai J, et al. Direct writing of three-dimensional Cu-based thermal flow sensors using femtosecond laser-induced reduction of CuO nanoparticles[J]. Journal of Micromechanics and Microengineering, 2017, 27(5): 055013.

[84] Mizoshiri M, Ito Y, Arakane S, et al. Direct fabrication of Cu/Cu_2O composite micro-temperature sensor using femtosecond laser reduction patterning [J]. Japanese Journal of Applied Physics, 2016, 55 (6S1): 06GP05.

Direct Laser Writing of Micro/Nano Copper Structures and Their Applications

Zhou Xingwen, Liao Jianing, Yao Yu, Kang Hui, Guo Wei, Peng Peng*

School of Mechanical Engineering & Automation, Beihang University, Beijing 100191, *China*

Abstract

Significance Owing to excellent adaptability to different working conditions, flexible electronics have attracted significant attention in many fields, such as wireless communication, human-machine interaction, and personal healthcare. Functional parts and conductive circuits are the basic components of electronics that respond to external stimulus and conduct signals, respectively.

Nanomaterials with unique physical and chemical properties are widely used for developing flexible electronics. Noble metals, such as silver, gold, and platinum are good candidates for manufacturing conductive parts because of their high conductivity and chemical stability. However, the high price of these metals limits their large scale production. Recently, copper has been considered a good alternative to noble metals for developing conductive component owing to its low-cost and excellent electrical properties. Furthermore, copper oxides (cuprous oxide and cupric oxide) are important transition metal oxides because of their semiconductive properties. They have been widely used as functional parts owing to their high sensitivity for external stimulation, such as humidity, temperature. Efficient manufacturing methods for materials play a major role in developing high-performance devices.

The typical "bottom-up" process, such as hydrothermal and chemical precipitation, provides a low-cost, precise control, and large-scale synthesis route to manufacture the micro/nanostructured copper. However, post-treatment processes, such as printing and sintering, are required to obtain the desired properties in a device. Such step-by-step manufacturing requires the cooperation of various techniques, which increases the process cost and complexity. Thus, developing a low-cost process for manufacturing the micro/nanostructures has attracted significant attention.

Direct laser writing, as an advanced processing technology developed recently, provides a novel approach for micro/nanostructure manufacturing. This technology has been used to process the structure, including noble metals, metal oxides, and carbon-based materials. In this study, the technical characteristics of manufacturing copper-based micro/nanostructures with direct laser writing have been summarized.

Progress The typical laser processing of micro/nanostructures, such as laser assembly, sintering, and synthesis, has been elaborated (Fig. 1). The advantages of laser processing compared with other processing technologies are presented. Then, the studies of laser sintering, reduction, and synthesis, for manufacturing copper structures are reviewed. The challenges of laser processing for copper-based materials, especially for the conductive copper structure, are highlighted. Subsequently, one-step direct laser writing technology based on the ionic precursor has been discussed. The typical manufacturing process and mechanism of the one-step direct laser writing of copper structures are revealed (Fig. 2). The effects of process parameters, such as precursor compositions, reducing agent type, laser wavelength, and laser parameters on the structure and electrical properties of patterns are discussed (Fig. 3). The tuning methods of the copper micro/nanostructures, such as topography, composition, and joining behavior during the writing process are demonstrated. The conductivity of the written structure and its influencing factors, such as porosity and composition, are comprehensively summarized according to the previously reported

studies (Fig. 4). Besides, the manufacturing method of antioxidation copper structures with direct laser writing is described (Fig. 5). Typical applications of the copper-based structures in conductive (Fig. 6) and functional parts (Fig. 7) in microelectronic devices are listed. The working mechanisms of these typical devices, such as an electrode, antenna, heater, capacitor, and sensors, and their influencing factors in performance have been clarified. Finally, the development trend of laser direct writing of micro/nano copper structures has prospected.

Conclusions and Prospect In summary, direct laser writing has been an efficient manufacturing process for copper micro/nanostructures owing to its noncontact, maskless, and rapid processing characteristics. Direct laser writing based on ionic precursors integrates the synthesis, positioning, assembly, and joining of copper nanomaterials into a one-step, which shows unique advantages in structure and composition control. This process still faces challenges in processing copper structures, such as the accurate control of products, diversification of composite structures, and further expansion of application. Further, in-depth study is needed to explore the writing mechanism and fully understand the processing characteristics for copper-based micro/nanostructures.

Key words laser manufacture; laser materials processing; nanomaterials; nanojoining; flexible electrode

OCIS codes 140.3390; 140.3450; 160.4236